

See discussions, stats, and author profiles for this publication at: <https://www.researchgate.net/publication/244424972>

# Adsorption of N x O y Based Molecules on Large Water Clusters: An Experimental and Theoretical Study

ARTICLE *in* THE JOURNAL OF PHYSICAL CHEMISTRY A · FEBRUARY 1997

Impact Factor: 2.69 · DOI: 10.1021/jp962213+

CITATIONS

9

READS

23

7 AUTHORS, INCLUDING:



**Maisa Ahmed**

An-Najah National University

34 PUBLICATIONS 535 CITATIONS

SEE PROFILE



**Ian H Hillier**

The University of Manchester

566 PUBLICATIONS 10,622 CITATIONS

SEE PROFILE



**John Christopher Whitehead**

The University of Manchester

155 PUBLICATIONS 2,272 CITATIONS

SEE PROFILE

# Adsorption of $N_xO_y$ -Based Molecules on Large Water Clusters: An Experimental and Theoretical Study

M. Ahmed, C. J. Apps, R. Buesnel, C. Hughes, I. H. Hillier,\* N. E. Watt, and J. C. Whitehead\*

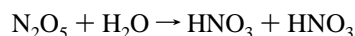
Department of Chemistry, University of Manchester, Manchester M13 9PL, U.K.

Received: July 23, 1996; In Final Form: December 5, 1996<sup>®</sup>

The sticking efficiencies for a range of  $N_xO_y$  species ( $NO$ ,  $NO_2$ ,  $N_2O$ ,  $N_2O_5$ , and  $HNO_3$ ) onto large water clusters have been studied using a supersonic molecular beam expansion to generate water clusters containing 50–450 water molecules.  $NO$ ,  $NO_2$ , and  $N_2O$  are found to stick with very low efficiencies relative to the organic species studied previously. This is in accord with studies for the corresponding species performed on cooled water ice films. In contrast,  $N_2O_5$  is efficiently converted to nitric acid by a heterogeneous surface reaction with the water cluster. Quantum mechanical–molecular dynamics calculations of the energies for the interaction of  $NO$ ,  $NO_2$  and  $N_2O$  with a water molecule and a small water cluster,  $(H_2O)_{10}$ , have been performed. These show that the  $NO_x$  molecule prefers to be bonded to the surface of the cluster and that it boils off the cluster at 140 K.

## Introduction

The chemistry of nitrogen oxide species is important in relationship to the formation and destruction of ozone in the stratosphere. In addition to a range of gas-phase processes, there is considerable interest in the heterogeneous processes taking place on the surface of polar stratospheric cloud (PSC) ice particles. Such processes are responsible for the creation of chlorine-containing species ( $HOCl$ ,  $ClNO_2$ , and  $Cl_2$ ) that can be photolyzed in the polar spring to give active chlorine, which can destroy ozone. Particles containing nitric acid can denitrify the stratosphere by sedimentation reducing the possibility for converting active chlorine species into inert reservoir compounds in the polar spring. Of particular interest is the heterogeneous reaction of  $N_2O_5$  with stratospheric ice particles to produce nitric acid



In this paper, we report results for the accommodation of some  $N_xO_y$  species ( $NO$ ,  $NO_2$ ,  $N_2O$ ,  $N_2O_5$ , and  $HNO_3$ ) by large water clusters generated in a supersonic molecular beam expansion. The  $N_xO_y$  molecule is deposited onto the cluster after the expansion is completed using the pickup technique. A mass spectrometric study of the final state of the cluster yields information about the relative sticking efficiency and the extent of any reaction. Preliminary results for the sticking of  $N_2O_5$  have been reported.<sup>1</sup> We have also performed calculations of the interaction energies for  $NO$ ,  $NO_2$ , and  $N_2O$  with a water molecule and with a small water cluster,  $(H_2O)_{10}$ , to aid the interpretation of our results.

## Experimental Section

The experimental procedures employed in this experiment are identical with those reported in the preceding paper.<sup>2</sup> A beam of large water clusters ( $\bar{n} \sim 50$ –450) was produced by a supersonic expansion of pure water vapor ( $P_0 < 2$  bar) through a 0.3 mm conical nozzle. Under these conditions, the water clusters have been shown by electron diffraction to be amorphous with an internal temperature that approaches a limiting

value of  $\sim 180$  K for the larger clusters.<sup>3</sup> Time-of-flight spectroscopy for the monomers and small water clusters in the beam ( $n < 16$ ) indicate that the translational temperature is  $\sim 105$  K.<sup>4</sup> Small clusters are formed by three-body collisions and are relatively cold, while the larger clusters arise from coalescence due to cluster–cluster collisions and are stabilized by evaporative cooling which gives rise to a higher temperature.<sup>5</sup> Under our conditions, the beam composition is made up of large clusters whose size is controlled by the water stagnation pressure and the corresponding size distribution is bell-shaped, peaking at  $\bar{n}$  with a full width at half-maximum of  $\sim \bar{n}$ .<sup>4</sup>

At 15 mm downstream from the nozzle, the cluster beam was crossed by an effusive spray from the pickup source operating at pressures  $< 8$  mbar. After passing through two further stages of differential pumping and being modulated by a tuning fork chopper, the beam was detected by a quadrupole mass spectrometer (0–300u) employing electron-impact ionization with an electron energy of 70 eV. Modulation was employed to improve the signal-to-noise of the mass spectrum by distinguishing between the signal from the beam and the residual background in the mass spectrometer. Reduction of the electron energy to  $< 10$  eV does not affect the mass spectral cracking patterns (the relative ratios of the ion peaks) although the overall intensity of the mass spectrum is reduced.

The sticking of the following  $N_xO_y$ -based compounds onto the water clusters was investigated: nitric oxide, nitrous oxide, nitrogen dioxide, nitric acid, and dinitrogen pentoxide. Nitric oxide ( $> 99\%$ ), nitrous oxide ( $> 99.5\%$ ), and nitrogen dioxide ( $> 99.5\%$ ) (Argo International) were introduced into the pickup source from a lecture bottle via a regulator and needle valve. The nitric oxide was tested for any  $NO_2$  or  $N_2O$  impurities by infrared spectroscopy which showed no trace of either gas allowing an upper limit of 1% to be placed upon their presence in the sample. Nitric acid was prepared from fuming nitric acid ( $> 95\%$ , Fisons) under vacuum by repeated freeze–pump–thaw cycles to remove the residual  $NO_2$  until the ratio of the  $NO^+$  to  $NO_2^+$  peaks in the mass spectrum was constant and the mass spectrum agreed with that of Jochims et al.<sup>6</sup> The nitric acid was stored in a glass ampule and run at room temperature.  $N_2O_5$  was prepared by the method of Davidson et al.<sup>7</sup> except that  $NO_2$  rather than  $NO$  was used for the oxidation to  $N_2O_5$  by ozone.

<sup>®</sup> Abstract published in *Advance ACS Abstracts*, January 15, 1997.

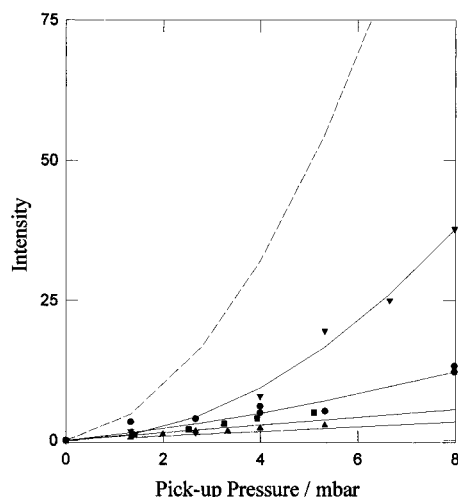


**Figure 1.** Variation of the relative intensity of the adsorbed molecules versus pickup source pressure for a water stagnation pressure of  $\sim 1.2$  bar ( $\bar{n} \sim 200$ ). (■) NO; (●) N<sub>2</sub>O; (▼) HNO<sub>3</sub>; (▲) NO<sub>2</sub>. The dashed curve represents the corresponding curve for the sticking of methanol (from ref 2).

**TABLE 1: Sticking Efficiencies for the Various Species onto a Water Cluster ( $\bar{n} \sim 200$  Molecules) Expressed Relative to the Efficiency for Methanol, Evaluated for a Pickup Pressure of 5 mbar<sup>a</sup>**

| pickup molecule                     | relative sticking efficiency | mean no. of molecules, $\bar{m}$ , picked up |
|-------------------------------------|------------------------------|--|
| nitrogen dioxide (NO <sub>2</sub> ) | 0.05                         | 1.0  |
| nitric oxide (NO)                   | 0.09                         | 1.0  |
| nitrous oxide (N <sub>2</sub> O)    | 0.15                         | 1.2  |
| nitric acid (HNO <sub>3</sub> )     | 0.29                         | 2.0  |
| methanol (CH <sub>3</sub> OH)       | 1.0                          | 1.8  |

<sup>a</sup> The mean number of molecules of each species,  $\bar{m}$ , attached to the water cluster is also listed. The data for methanol comes from ref 2.

Ozone was generated by passing dry, high-purity oxygen through a commercial ozonizer. The N<sub>2</sub>O<sub>5</sub> was stored under vacuum at  $-80$  °C between experiments and run from a glass ampule in a salt/ice bath. The purity of the N<sub>2</sub>O<sub>5</sub> was confirmed from its mass spectrum.

## Experimental Results

As in the previous study,<sup>2</sup> the efficiency of the pick-up process for the various gases was determined by monitoring with the quadrupole mass spectrometer, the intensity of the principal ion peak for the appropriate molecule as a function of pickup source pressure at a given water stagnation pressure. The results for NO, NO<sub>2</sub>, N<sub>2</sub>O, and HNO<sub>3</sub> are shown in Figure 1 for a water stagnation pressure of  $\sim 1.2$  bar, corresponding to a cluster size of  $\bar{n} \sim 200$  water molecules. The data have been corrected for any variation in the flux of the water cluster beam and for the relative ionization efficiencies of the different molecules. The various results have been normalized to those for methanol. It can be seen that all these molecules stick with relatively low efficiency compared to methanol, particularly NO and NO<sub>2</sub>. Using the methods discussed in the previous paper<sup>2</sup> which involve the fitting of the curves in Figure 1 to a quadratic function in the pickup source pressure, we can obtain values for the sticking efficiencies of these molecules relative to methanol at a given pressure. These values are given in Table 1 together with the mean number of molecules,  $\bar{m}$ , picked-up by each water cluster. To confirm that it was NO<sub>2</sub> rather than N<sub>2</sub>O<sub>4</sub> that was deposited onto the water cluster, experiments were performed with the pickup source outlet tube heated to 100 °C, and the results were compared with those taken with

the tube at its normal room-temperature conditions. There was no difference in the form of the intensity versus pickup source pressure curve recorded under both conditions. Thus, we conclude that it is NO<sub>2</sub> and not N<sub>2</sub>O<sub>4</sub> that has been attached to the water cluster in these experiments. Additional experiments were performed in which the intensity of the principal ion peak for the N<sub>x</sub>O<sub>y</sub> species versus pickup pressure was measured for various water source stagnation pressures. No differences were found in the form of these curves as a function of stagnation pressure, indicating that the efficiency of the pickup process is independent of the size of the water cluster, for the range studied here (50–450 molecules per cluster).

For NO, NO<sub>2</sub>, N<sub>2</sub>O, and HNO<sub>3</sub>, it was found that the cracking pattern of the mass spectrum for the molecule when attached to the water cluster was identical with that for the isolated gas-phase molecule as was noted previously for the organic molecules.<sup>2</sup> These species have ionization potentials that are comparable to or lower than that for water and based on our previous experience with organic species,<sup>2,8</sup> it is assumed that they are directly ionized and detach rapidly from the water cluster without undergoing any ion–molecule collisions with the cluster. The mechanism of ionization will be further discussed below.

However, it was not possible to adopt the above procedure for the analysis of the data for the sticking of N<sub>2</sub>O<sub>5</sub> onto the water clusters because the mass spectrum for the N<sub>2</sub>O<sub>5</sub> was found to change with pickup source pressure, although it is possible to determine that the sticking efficiency lies in the range 0.4–0.8 relative to methanol. Figure 2 shows the comparison between the mass spectra for gas-phase N<sub>2</sub>O<sub>5</sub> and for N<sub>2</sub>O<sub>5</sub> attached to a water cluster. Also shown for comparison is the corresponding mass spectrum for nitric acid attached to a water cluster. The figure shows that there has been a clear change from the fragmentation pattern associated with pure gas-phase N<sub>2</sub>O<sub>5</sub> (upper panel) upon attachment of the N<sub>2</sub>O<sub>5</sub> onto the water cluster (middle panel). Specifically, there is a reversal of the ordering of the relative intensities of the NO<sup>+</sup> to NO<sub>2</sub><sup>+</sup> ion peaks following accommodation to give a fragmentation pattern which is essentially identical with that resulting from the direct attachment of HNO<sub>3</sub> onto a water cluster (lower panel). It is clear that the N<sub>2</sub>O<sub>5</sub> has been converted into nitric acid upon being attached to the water cluster. From the ratio of the intensities of the NO<sup>+</sup> to NO<sub>2</sub><sup>+</sup> ion peaks, we estimate that at least 80% of the N<sub>2</sub>O<sub>5</sub> has been converted into HNO<sub>3</sub>. Some distortion of the mass spectrum occurs when the mass spectrometer is operated in a scanning mode which especially affects the more intense peaks, and this is evident in the monomer water peaks in Figure 2. (Accurate calibration of the mass scale indicates that only monomer peaks (up to H<sub>2</sub>O<sup>+</sup>) are observed and not protonated water, (H<sub>2</sub>O)H<sup>+</sup>.) This scanning mode is mainly used to obtain qualitative information at relatively low resolution for survey and display purposes. However, quantitative information, including the pickup efficiency curves of Figure 1, is generally obtained by manually tuning the mass spectrometer to a particular mass peak with the best obtainable resolution.

## Computational Details

The objective of the calculations was to examine the structure and energetics of NO, NO<sub>2</sub>, and N<sub>2</sub>O solvated in small water clusters. Structures were obtained using a molecular dynamics (MD) approach, and to avoid the use of empirical potentials, we chose a quantum mechanical method to evaluate the necessary energies and forces. The use of a semiempirical molecular orbital method allows the calculation to be carried

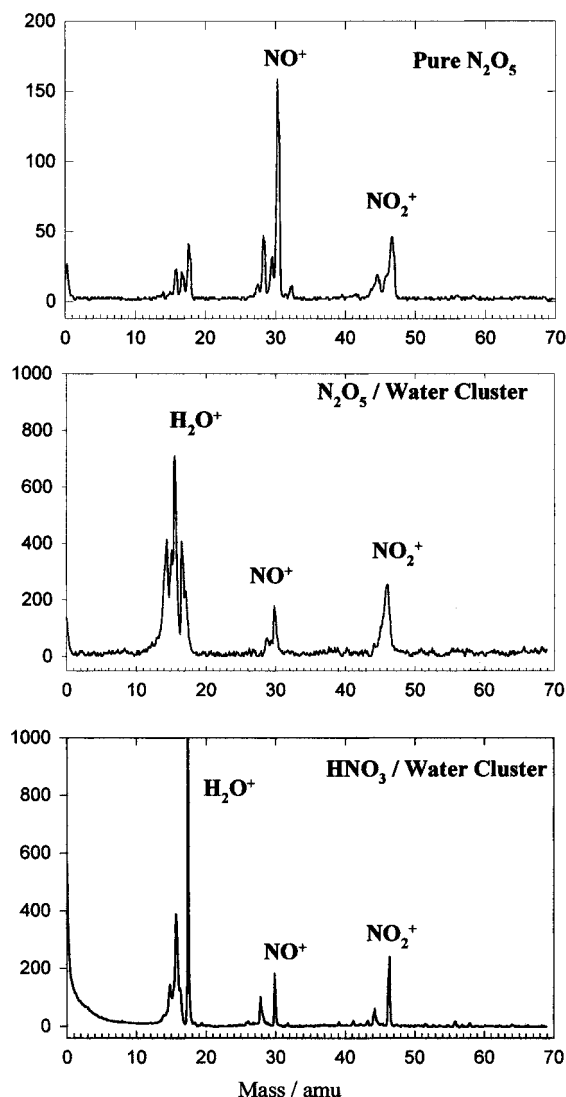


**Figure 2.** Comparison of the mass spectra for gas-phase N<sub>2</sub>O<sub>5</sub> (upper panel) with N<sub>2</sub>O<sub>5</sub> attached to a water cluster (middle panel) and with HNO<sub>3</sub> attached to a water cluster (lower panel). For the two lower spectra, the pick-up source pressure was 7 mbar and the water cluster were formed at a stagnation pressure of  $\sim 1.2$  bar ( $\bar{n} \sim 200$ ).

out in reasonable amounts of computer time. We chose the AM1 Hamiltonian, which has been found to be satisfactory for modeling hydrogen bonded interactions.<sup>9</sup> Simulations were carried out using traditional MD methods,<sup>10</sup> employing the Verlet algorithm<sup>11</sup> to integrate the Newtonian equations of motion and using the MOPAC program<sup>12</sup> to calculate the energies and forces. Low-energy structures were obtained using simulated annealing, employing the following protocol. For each system, a 10 ps simulation was carried out employing a time step of 1 fs. A starting structure was heated to 50 K (2 ps), equilibrated at this temperature (2 ps), and then cooled to 0 K (6 ps). This annealing procedure was carried out for a bare water cluster, (H<sub>2</sub>O)<sub>10</sub>, and one containing a single NO<sub>x</sub> solute molecule. In addition, H<sub>2</sub>O–NO<sub>x</sub> dimers were studied at the AM1 level using this simulated annealing technique and at the ab initio level (UMP2)<sup>13</sup> using a 6-31G\*\* basis. For the latter calculations, geometry optimization of the dimers was carried out starting with a variety of initial structures.

The results of the calculations are summarized in Table 2. For the dimers, both the semiempirical and ab initio calculations gave similar binding energies and both predict the order of the binding energies to be N<sub>2</sub>O > NO<sub>2</sub> > NO, with all three binding energies being considerably smaller than that predicted for

**TABLE 2: Results of the Simulations for NO, NO<sub>2</sub>, and N<sub>2</sub>O and Their Interactions with H<sub>2</sub>O and with (H<sub>2</sub>O)<sub>10</sub> Clusters, Using AM1 Hamiltonian**

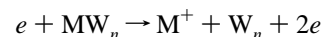
| system   | energy/ev   | binding energy <sup>a</sup> /kJ mol <sup>-1</sup> |
|--|-------------|---|
| dimers   |             |   |
| NO...H <sub>2</sub> O                            |             | 10.0 (10.9)                                       |
| NO <sub>2</sub> ...H <sub>2</sub> O              |             | 12.1 (12.3)                                       |
| N <sub>2</sub> O...H <sub>2</sub> O              |             | 14.2 (12.6)                                       |
| CH <sub>3</sub> OH...H <sub>2</sub> O            |             | 22.2  |
| clusters   |             |   |
| (H <sub>2</sub> O) <sub>10</sub>                 | -3489.0287  |   |
| NO(H <sub>2</sub> O) <sub>10</sub>               | -4015.18725 |   |
| NO   | -525.95277  | 19.7  |
| NO <sub>2</sub> (H <sub>2</sub> O) <sub>10</sub> | -4334.64471 |   |
| NO <sub>2</sub>                                  | -845.39097  | 21.8  |
| N <sub>2</sub> O(H <sub>2</sub> O) <sub>10</sub> | -4221.36459 |   |
| N <sub>2</sub> O                                 | -732.06377  | 26.4  |

<sup>a</sup> Ab initio (UMP2) values in parentheses.

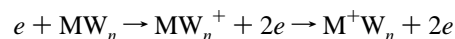
methanol. As far as the results for the clusters are concerned, the solute molecule migrated to the surface of the cluster during the simulation, despite initial structures being chosen having the solute at the center of the cluster. It is of interest that such behavior is frequently found in cluster simulations using both effective<sup>14,15</sup> and quantum mechanical potentials.<sup>16</sup> The calculated binding energies for the three solutes in the clusters follow the same trend as for the dimer, although, not unexpectedly, the values are somewhat larger due to additional NO<sub>x</sub>–water interactions. It is of interest to note that the MD simulations revealed that the NO, NO<sub>2</sub>, and N<sub>2</sub>O molecules all boiled-off from the water cluster at 140 K, whereas CH<sub>3</sub>OH did not boil off for temperatures up to 200 K, in line with the greater binding energy of the latter species.

## Discussion

In these studies, it is important to be able to relate the observed mass spectrum to the properties of the neutral cluster and the processes resulting upon electron impact ionization. This will depend on many factors such as the size of the cluster, its temperature, the relative concentrations of the species, whether the molecule is in the bulk of the cluster or resides upon the surface, the electron energy, and the relative ionization potentials of the species in the cluster. The dominant ion peaks of low mass that we observe in this work consist of ionized water monomer peaks and the unprotonated picked-up molecule. It is appropriate to discuss the likely processes that may occur upon the ionization of a large water cluster, W<sub>n</sub>, containing an added molecule, M. For the case when the ionization potential of the adduct molecule, M, is less than the ionization potential of a water molecule which is the most common case for the molecules studied here, it is possible to get direct ionization of the adduct:

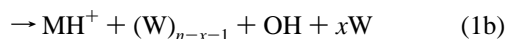
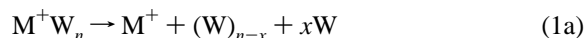


as was suggested previously.<sup>2,8</sup> However, because of its size, the large water cluster presents a much greater cross section for ionization than the single adduct molecule despite the higher ionization potential for water. In this case, the water host will be ionized and the charge will migrate through the water cluster and transfer to the molecule, M:



In their pickup experiments forming small mixed clusters, Stace and co-workers<sup>17,18</sup> have demonstrated with infrared spectroscopy that the charge ultimately resides on the species

with the lowest ionization potential. The ionized cluster, M<sup>+</sup>W<sub>n</sub>, may then release its excess energy either by direct detachment and evaporation of the ion from the cluster or by an intracuster ion–molecule reaction followed by prompt fragmentation of the cluster:

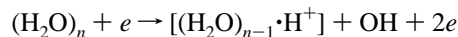


In both cases, the resulting ion may also be hydrated. This behavior was observed by us for the ionization of methanol picked-up by large water clusters,<sup>8</sup> although the intensities of the hydrated and protonated peaks were much less than those for the unprotonated parent methanol. The absence of such peaks in the present work may result from their low intensity compared with the detection sensitivity of our quadrupole mass spectrometer.

Toennies and co-workers have investigated the electron impact ionization of single SF<sub>6</sub> molecules picked up by large liquid helium clusters containing several thousand atoms.<sup>19</sup> Initially, a surface helium atom is ionized followed by resonant charge transfer until the charge becomes located upon the SF<sub>6</sub> when the energy released leads to an explosive fragmentation of the cluster in its entirety. Because of the liquid nature of the helium cluster, the picked up SF<sub>6</sub> molecule is located within the bulk of the cluster. However, corresponding experiments with large solid Ne clusters<sup>19</sup> where the SF<sub>6</sub> resides on the surface of the cluster give an SF<sub>6</sub> ion fragmentation pattern that is similar to that of a free SF<sub>6</sub> molecule. It is suggested that this results from direct ionization of the SF<sub>6</sub> because of its surface site rather than charge transfer from ionized Ne. The intensity of SF<sub>6</sub> ionization is much lower from the neon cluster than that observed for the helium cluster probably because the direct ionization of SF<sub>6</sub> on a neon cluster has a much lower cross section than that for ionization of the large helium cluster followed by charge transfer to the SF<sub>6</sub>. Garvey<sup>20</sup> has shown that the electron impact ionization of methanol–argon clusters is very dependent upon the size of the cluster. It appears that for large clusters, dissociative ionization of the methanol from the cluster surface dominates over intracuster ion–molecule reactions which give rise to protonated peaks, i.e., the rate of process 1a is faster than that of process 1b. Similar observations are reported for large argon–benzene clusters.<sup>21</sup>

Stace and co-workers have studied the production of the hydrated cluster ions, N<sub>x</sub>O<sub>y</sub>·(H<sub>2</sub>O)<sub>n</sub> (*n* ≤ 8), which they can produce with high yield by electron bombardment using the pickup method with NO<sup>22</sup> and NO<sub>2</sub>.<sup>23</sup> This is in contrast to our results where we fail to observe such hydrated ions. However, there is an important difference in the experimental arrangement adopted by Stace's group compared to the present study. They produce the water clusters by a supersonic expansion of water vapor entrained in a high pressure of argon gas. This gives a relatively small size distribution of water clusters which are predominantly in the form of heteroclusters, (H<sub>2</sub>O)<sub>n</sub>·Ar<sub>m</sub>. They find that the presence of argon in these clusters is especially beneficial to the pickup process as the weakly bound argon is preferentially evaporated from the resulting N<sub>x</sub>O<sub>y</sub>·(H<sub>2</sub>O)<sub>n</sub>·Ar<sub>m</sub> cluster giving rise to its stabilization. This forms a cooler cluster than results from our use of pure water vapor to form large water clusters. It is also quite likely that not all the argon atoms are evaporated from the resulting cluster before it is ionized and that any remaining argon is again preferentially evaporated upon ionization to enhance the formation of hydrated cluster ions, N<sub>x</sub>O<sub>y</sub>·(H<sub>2</sub>O)<sub>n</sub><sup>+</sup> rather than direct dissociative ionization of N<sub>x</sub>O<sub>y</sub>.

The absence of protonated water peaks and small clusters of water in our mass spectra can be explained by considering the size distribution and the mechanism of electron impact ionization of large water clusters. As mentioned previously, the composition of the water cluster beam consists of unclustered monomers and large clusters with a Gaussian size distribution.<sup>4</sup> The water monomers will ionize to give H<sub>2</sub>O<sup>+</sup> as the heaviest ion, while the large water clusters will give a protonated cluster upon ionization:



This ion may stabilize by evaporation of some water molecules, but as Lee<sup>24</sup> has shown the number is small for large water clusters. Thus ion peaks resulting from the ionization of our large water clusters will fall outside of our detectable mass range (<300u).

In summary, the ionization patterns that we observe indicate that ionization of the single molecular species that has been placed on the surface of the large solid water cluster by the pickup technique takes place either by the direct dissociative ionization of the molecule from the cluster or that ionization is of a water molecule followed by charge transfer across the cluster surface to the molecule. This results in the formation of the molecular ion which is rapidly evaporated from the water cluster which itself may be significantly fragmented. It would appear from our results that this evaporation–fragmentation process occurs more rapidly than the competing intracuster ion–molecule reaction. It would be interesting to see if this hypothesis can be confirmed by model calculations of the doping and subsequent ionization of water clusters.

With the exception of nitric acid which sticks onto the water clusters with an efficiency comparable to benzene, all the nonreactive N<sub>x</sub>O<sub>y</sub> species have very low sticking efficiencies compared to the organic species studied previously<sup>2</sup> where relatively strong hydrogen bonding to the “dangling” OH bonds was responsible for the adsorption. The low sticking efficiencies seen for the N<sub>x</sub>O<sub>y</sub> species on the water clusters are similar in their ordering with those observed for the same species on cold water ice films. Saastad et al.<sup>25</sup> could find no significant adsorption of NO and NO<sub>2</sub> on water ice in the temperature range 193–243 K and placed an upper limit of 5 × 10<sup>−5</sup> on the uptake coefficient. At lower temperatures (~100 K), Rieley et al.<sup>26</sup> found that the sticking coefficient for NO<sub>2</sub> on ice increases with decreasing temperature and that the accommodated NO<sub>2</sub> dimerizes to N<sub>2</sub>O<sub>4</sub>. They found that the desorption temperature is ~145 K, which is very close to the temperature above which our calculations indicated that NO, NO<sub>2</sub>, and N<sub>2</sub>O would boil off the (H<sub>2</sub>O)<sub>10</sub> cluster. Nitric acid is found<sup>27</sup> to have a more efficient uptake on water ice with an accommodation coefficient of ≥0.3 at 191.5 K.

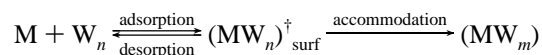
While the reaction of N<sub>2</sub>O<sub>5</sub> with water is very slow in the gas phase (*k* < 2.8 × 10<sup>−21</sup> cm<sup>3</sup> molecule<sup>−1</sup> s<sup>−1</sup>),<sup>28</sup> the probability for the heterogeneous reaction of N<sub>2</sub>O<sub>5</sub> on water ice is ~0.024,<sup>29</sup> although the surface rapidly becomes less reactive as it becomes covered with nitric acid. Quinlan et al.<sup>30</sup> find that N<sub>2</sub>O<sub>5</sub> is quantitatively converted to nitric acid on an ice surface at 188 K. They suggest that the reaction is acid catalyzed and the subsequent buildup of a nitric acid surface layer quenches the autocatalysis. Horn et al.<sup>31</sup> have studied the reaction of N<sub>2</sub>O<sub>5</sub> on water ice at 80–160 K and identified molecular nitric acid and nitric acid hydrate at 160 K by infrared spectroscopy. They concluded that the reaction of gas-phase N<sub>2</sub>O<sub>5</sub> with ice, proceeds via ionic chemistry involving nitrate, nitronium, and hydroxonium ions. The ionic chemistry involved has been further investigated in a study<sup>32</sup> of N<sub>2</sub>O<sub>5</sub> with

protonated water clusters  $\text{H}^+(\text{H}_2\text{O})_n$  where reaction to form clusters containing nitric acid  $\text{H}^+(\text{H}_2\text{O})_n(\text{HNO}_3)_m$  takes place for clusters with  $n \geq 5$  and at temperatures below 160 K. Ionic chemistry involving protonated water clusters has also been investigated for nitric acid,<sup>33,34</sup> where it was shown that reaction of nitric acid with protonated water clusters gives  $\text{H}^+(\text{H}_2\text{O})_n(\text{HNO}_3)$  for  $n \geq 5$  via a fast proton transfer and that  $\text{NO}_2^+(\text{H}_2\text{O})_n$  is the most stable form of hydrated nitric acid for small values of  $n$  ( $\leq 3$ ). Similarly, the formation of nitrous acid ( $\text{HONO}$ ) and protonated, hydrated nitrous acid from  $\text{NO}^+(\text{H}_2\text{O})_n$  has been studied.<sup>22,35</sup>

Rieley et al.<sup>26</sup> found no evidence for reaction of  $\text{NO}_2$  and the water surface in their studies of the adsorption of  $\text{NO}_2$  onto ice films at  $\sim 100$  K and determined that the adsorbed species is in fact  $\text{N}_2\text{O}_4$  oriented with the N–N bond perpendicular to the surface. Mertes and Wahner<sup>36</sup> have studied the uptake of  $\text{NO}_2$  on aqueous surfaces at 298 K finding a mass accommodation coefficient of  $\geq 2 \times 10^{-4}$ . They suggest that  $\text{NO}_2$  dimerizes on the surface of the water and a surface reaction produces both nitrous and nitric acid. It would seem that dimerization of  $\text{NO}_2$  on either a solid or liquid water surface occurs readily and may be a necessary prerequisite for any surface reaction. In our studies, the average number of  $\text{NO}_2$  molecules picked up is one that is insufficient for dimerization and any further reaction; this may account for the low sticking efficiency that we measure.

For the organic species a strong correlation was found between the molecule–water interaction energy and the relative sticking efficiency. There is a paucity of information about the corresponding interaction energies between the  $\text{N}_x\text{O}_y$  species and water which was the driving force for our theoretical studies for  $\text{NO}$ ,  $\text{NO}_2$ , and  $\text{N}_2\text{O}$  and a single water molecule and small water clusters. For the heterodimer interactions ( $\text{N}_x\text{O}_y\text{--H}_2\text{O}$ ), the calculations indicate that the interaction energies are all very similar lying between 10 and 14  $\text{kJ mol}^{-1}$ , with the ordering being  $\text{NO} < \text{NO}_2 < \text{N}_2\text{O}$ . From the correlation determined for the organic species, we would expect the sticking efficiencies for  $\text{NO}$ ,  $\text{NO}_2$ , and  $\text{N}_2\text{O}$  to lie in the range 0.35–0.50 relative to methanol. In fact, the observed values are in the range 0.05–0.15 for these species and the experimental ordering of the sticking efficiencies ( $\text{NO}_2 < \text{NO} < \text{N}_2\text{O}$ ) reverses the ordering of  $\text{NO}$  and  $\text{NO}_2$  compared with the calculations. Clearly, considerations other than just interaction energies must also apply when discussing the adsorption of these species to the water clusters.

We consider a two-stage mechanism where a molecule,  $\text{M}$ , is attached to a water cluster,  $\text{W}_n$ :



The first step corresponds to the adsorption of the molecule onto the cluster to give an energized surface intermediate state,  $(\text{MW}_n)^{\dagger}_{\text{surf}}$ . If the binding of the molecule is large enough, the heat of adsorption will be dissipated in the cluster by the evaporation of a small number of molecules stabilizing the cluster. For large enough clusters, this additional energy can be accommodated without any melting of the cluster. This mechanism is responsible for the binding of the organic molecules to the water clusters and gives rise to the observed correlation of sticking efficiency with binding energy. For the more weakly bound species, desorption from the cluster will become an important process. Our calculations show that the  $\text{NO}_x$  molecules boil off the surface of the cluster for temperatures greater than 140 K, while methanol remains attached up to 200 K. Desorption will dominate unless there is some competing mechanism that gives rise to accommodation of the molecule

within the cluster. This could arise from solvation of the molecule or from a surface reaction of the adsorbed molecule with the cluster. This mechanism is analogous to precursor-mediated adsorption in gas–surface interactions where there is a weak physisorbed precursor state that is separated from a stronger adsorbed state by an energy barrier. It is possible that in the case of  $\text{NO}$ ,  $\text{NO}_2$ , and  $\text{N}_2\text{O}$ , a relatively large barrier separates the weakly bound precursor state from the more strongly bound adsorbed state that is given by the calculations accounting for the relatively low sticking efficiencies observed in the experiment.

Clearly, reaction is responsible for the accommodation of  $\text{N}_2\text{O}_5$  by the water cluster as is confirmed by the observation of the end product, nitric acid. This gives a higher sticking coefficient relative to the other  $\text{N}_x\text{O}_y$  species. Nitric acid is also effectively adsorbed to the cluster, but it is not clear to what extent it might be solvated or dissociated. In the preceding paper,<sup>2</sup> we demonstrated that in the pickup experiments involving the organic species, the molecules remained adsorbed onto the surface and did not become incorporated (or solvated) within the bulk of the cluster. Part of the evidence for this conclusion was that the mass spectral cracking patterns for the molecules picked up by the water cluster were unchanged from those for the isolated gas-phase molecules, and there was thus no evidence of any significant interaction or transformation. This is the case for all the  $\text{N}_x\text{O}_y$  species except for  $\text{N}_2\text{O}_5$ . Our calculations show a similar behavior for the binding of  $\text{NO}$ ,  $\text{NO}_2$ , and  $\text{N}_2\text{O}$  to the  $(\text{H}_2\text{O})_{10}$  water cluster where the molecule prefers to remain on the surface of the clusters rather than being surrounded by a shell of water molecules. There is an increase in stability of about a factor of 2 in the case of binding to the cluster compared with binding to a single water molecule due to the increased number of interactions which we have described as being the “solvation energy” (Table 2). Some localized solvation may occur, but this will only be within the surface layer and not in the bulk. Both  $\text{NO}$  and  $\text{N}_2\text{O}$  are only slightly soluble in liquid water (7.34 and 130  $\text{cm}^3/100 \text{ cm}^3$  of water at 0 °C, respectively) while  $\text{NO}_2$  is soluble and decomposes to give nitric acid. However, we find that these species are only weakly adsorbed onto the amorphous surface of our large water clusters in agreement with the corresponding results for ice films.

A final comment relates to how representative water clusters might be as a mimic for polar stratospheric cloud ice particles. The water clusters are significantly smaller than stratospheric ice particles with diameter of  $\sim 10$  nm compared with  $\sim 10 \mu\text{m}$  for PSC type II ice particles. However, the clusters do possess the correct surface morphology, dimensionality, and temperature to be representative of ice particles and are also formed by the process of nucleation. Our studies of the dependence of the sticking upon the cluster size showed no size dependence, albeit over a limited range. The major difference relates to the nature of the gas–surface interaction in the pickup region compared with the corresponding process in the stratosphere. In the pickup region, the gas–surface interaction is limited to a short period of time determined by the time-of-flight of the cluster beam through the pickup region ( $\sim 20 \mu\text{s}$ ). In contrast, polar stratospheric ice particles are in contact with a low partial pressure of the molecule in question ( $\sim 1 \times 10^9 \text{ molecules cm}^{-3}$ ) for extended periods of time allowing an equilibrium to be established between molecules in the gas phase and those on the surface and allowing for diffusion to and from the surface into the bulk of the ice crystal. In our experiment, we do not get extensive coverage of the surface as only one or two molecules on average are picked up, and we do not then experience effects due to the release of large amounts of energy

associated with the heat of adsorption which can give rise to melting and significant solubility of the molecules and the consequent ionic chemistry. We do, however, isolate and probe the initial interactions between the molecule and the cluster.

**Acknowledgment.** This work was supported by the Nuffield Foundation, EPSRC and NERC. We thank Dr. M. A. Vincent for carrying out the ab initio calculations.

## References and Notes

- (1) Ahmed, M.; Apps, C. J.; Hughes, C.; Watt, N. E.; Whitehead, J. C. *Faraday Discuss. Chem. Soc.* **1995**, *100*, 341.
- (2) Ahmed, M.; Apps, C. J.; Hughes, C.; Watt, N. E.; Whitehead, J. C. *J. Phys. Chem.*, preceding paper in this issue.
- (3) Torchet, G.; Schwartz, P.; Farges, J.; de Feraudy, M. F.; Raoult, B. *J. Chem. Phys.* **1983**, *79*, 6196.
- (4) Ahmed, M.; Apps, C. J.; Hughes, C.; Whitehead, J. C. *J. Phys. Chem.* **1994**, *98*, 12530.
- (5) Soler, J. M.; García, N.; Echt, O.; Sattler, K.; Recknagel, E. *Phys. Rev. Lett.* **1982**, *49*, 1857.
- (6) Jochims, H.-W.; Denzer, W.; Baumgärtel, H.; Lösling, O.; Willner, H. *Ber. Bunsen-Ges. Phys. Chem.* **1992**, *96*, 573.
- (7) Davidson, J. A.; Viggiano, A. A.; Howard, C. J.; Dotan, I.; Fehsenfeld, F. C.; Albriton, D. L.; Ferguson, E. E. *J. Chem. Phys.* **1978**, *68*, 2085.
- (8) Ahmed, M.; Apps, C. J.; Hughes, C.; Whitehead, J. C. *Chem. Phys. Lett.* **1995**, *240*, 216.
- (9) Dewar, M. J. S.; Zoebisch, E. G.; Healey, E. F.; Stewart, J. J. P. *J. Am. Chem. Soc.* **1985**, *107*, 3902.
- (10) Allen, M. P.; Tildesley, D. J. *Computer Simulation of Liquids*; Clarendon Press: Oxford, 1987.
- (11) Verlet, L. *Phys. Rev.* **1967**, *159*, 98.
- (12) Stewart, J. J. P. *J. Computer-Aided Mol. Design* **1990**, *4*, 1.
- (13) Hehre, W. J.; Radom, L.; Schleyer, P. v. R.; Pople, J. A. *Ab Initio Molecular Orbital Theory*; Wiley: New York, 1986.
- (14) Caldwell, J. W.; Kollman, P. A. *J. Phys. Chem.* **1992**, *96*, 8249.
- (15) Byers Brown, W.; Hillier, I. H.; Masters, A. J.; Palmer, I. J.; Dos Santos, D. H. V.; Stein, M.; Vincent, M. A. *Faraday Discuss. Chem. Soc.* **1995**, *100*, 253.
- (16) Buesnel, R.; Hillier, I. H.; Masters, A. J. *Chem. Phys. Lett.* **1995**, *247*, 391.
- (17) Jones, A. B.; Woodward, C. A.; Winkel, A. J.; Stace, A. J. *Int. J. Mass. Spectrom. Ion Processes* **1994**, *133*, 83.
- (18) Winkel, J. F.; Woodward, C. A.; Jones, A. B.; Stace, A. J. *J. Chem. Phys.* **1995**, *103*, 5177.
- (19) Scheidemann, A.; Schilling, B.; Toennies, J. P. *J. Phys. Chem.* **1993**, *97*, 2128.
- (20) Vaidyanathan, G.; Coolbaugh, M. T.; Garvey, J. F. *J. Phys. Chem.* **1992**, *96*, 1589.
- (21) Kamke, B.; Kamke, W.; Wang, Z.; Ruhl, E.; Brutschy, B. *J. Chem. Phys.* **1987**, *86*, 2525.
- (22) Stace, A. J.; Winkel, J. F.; Lopez Martens, R. B.; Upham, J. E. *J. Phys. Chem.* **1994**, *98*, 2012.
- (23) Stace, A. J.; Winkel, J. F.; Attrill, S. R. *J. Chem. Soc., Faraday Trans.* **1994**, *90*, 3469.
- (24) Vernon, M. F.; Krajnoviich, D. J.; Kwok, H. S.; Lisy, J. M.; Shen, Y. R.; Lee, Y. T. *J. Chem. Phys.* **1982**, *77*, 47.
- (25) Saastad, O. W.; Ellermann, T.; Nielsen, C. J. *Geophys. Res. Lett.* **1993**, *20*, 1191.
- (26) Rieley, H.; McMurray, D. P.; Haq, S. J. *Chem. Soc., Faraday Trans.* **1996**, *92*, 933.
- (27) Hanson, D. R. *Geophys. Res. Lett.* **1992**, *19*, 2063.
- (28) Hatakeyama, S.; Leu, M.-T. *J. Phys. Chem.* **1989**, *93*, 5784.
- (29) Hanson, D. R.; Ravishankara, A. R. *J. Geophys. Res.* **1991**, *96*, 5081.
- (30) Quinlan, M. A.; Reihs, C. M.; Golden, D. M.; Tolbert, M. A. *J. Phys. Chem.* **1990**, *94*, 3255.
- (31) Horn, A. B.; Koch, T.; Chesters, M. A.; McCoustra, M. R. S.; Sodeau, J. R. *J. Phys. Chem.* **1994**, *98*, 946.
- (32) Wincel, H.; Mereand, E.; Castleman, A. W. *J. Phys. Chem.* **1994**, *98*, 8606.
- (33) Cao, Y.; Choi, J.-H.; Haas, B.-H.; Johnson, M. S.; Okumura, M. *J. Chem. Phys.* **1993**, *99*, 9307.
- (34) Zhang, X.; Mereand, E. L.; Castleman, A. W. *J. Phys. Chem.* **1994**, *98*, 3554.
- (35) Choi, J.-H.; Kuwata, K. T.; Haas, B.-M.; Cao, Y.; Johnson, M. S.; Okumura, M. *J. Chem. Phys.* **1994**, *100*, 7153.
- (36) Mertes, S.; Wahner, A. *J. Phys. Chem.* **1995**, *99*, 14000.